BIOCHEMISTRY
including biophysical chemistry & molecular biology

Article

pubs.acs.org/biochemistry

Allosteric Activation and Contrasting Properties of L-Serine Dehydratase Types 1 and 2

Shawei Chen,[†] Xiao Lan Xu,[†] and Gregory A. Grant*[,†,‡]

[†]Department of Developmental Biology and [‡]Department of Medicine, Washington University School of Medicine, 660 South Euclid Avenue, Box 8103, St. Louis, Missouri 63110, United States

Supporting Information

ABSTRACT: Bacterial L-serine dehydratases differ from mammalian L- and D-serine dehydratases and bacterial D-serine dehydratases by the presence of an iron−sulfur center rather than a pyridoxyl phosphate prosthetic group. They exist in two forms, types 1 and 2, distinguished by their sequence and oligomeric configuration. Both types contain an ASB domain, and the type 1 enzymes also contain an ACT domain in a tandem arrangement with the ASB domain like that in type 1 D-3-phosphoglycerate dehydrogenases (PGDHs). This investigation reveals striking kinetic differences between L-serine dehydratases from *Bacillus subtilis* (*bs*LSD, type 1) and *Legionella pneumophila* (*lp*LSD, type 2). *lp*LSD is activated by monovalent cations and inhibited by monovalent anions. *bs*LSD is strongly activated by cations, particularly potassium, and shows a mixed response to anions. Flouride is a competitive inhibitor for *lp*LSD but an apparent activator for *bs*LSD at low concentrations and an inhibitor at high concentrations. The reaction products, pyruvate and ammonia, also act as activators but to different extents for each type. Pyruvate activation is competitive with L-serine, but activation of the enzyme is not compatible with it simply competing for binding at the active site and suggests the presence of a second, allosteric site. Because activation can be eliminated by higher levels of L-serine, it may be that this second site is actually a second serine binding site. This is consistent with type 1 PGDH in which the ASB domain functions as a second site for substrate binding and activation.

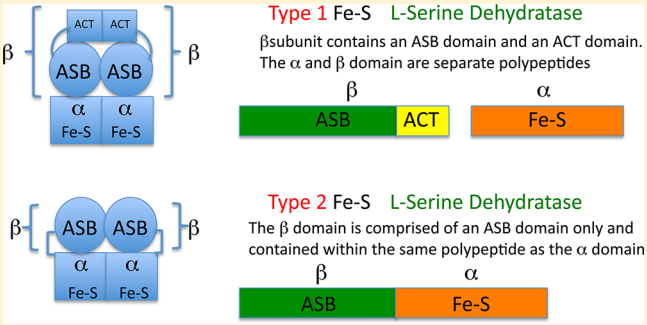

L-Serine dehydratases (EC 4.3.1.17) convert L-serine to pyruvate and ammonia.[1,2] All known bacterial L-serine dehydratases contain an iron−sulfur cluster at their catalytic site.[2−7] In contrast, mammalian L-serine dehydratases[8,9] and bacterial D-serine dehydratases[10,11] function by way of a pyridoxal 5′-phosphate (PLP) prosthetic group.

It has recently been shown[12,13] that when the L-serine dehydratase activity in *Escherichia coli* is knocked out, significant morphological abnormalities and cell lysis are observed. These studies resulted in the proposal that high serine levels decrease the level of synthesis of UDP-*N*-acetylmuramate-L-alanine by interfering with the *mur*C-encoded ligase. Thus, the role of these dehydratases may be to maintain the intracellular L-serine concentration at viable levels. However, they must do so without also depleting the intracellular level of L-serine to unsustainable levels.

Two types of L-serine dehydratases have been identified in bacteria, termed types 1 and 2,[14] shown schematically in Figure 1. Both types consist of a catalytic domain where the Fe−S center resides and a separate domain whose function has not yet been determined. In type 1 L-serine dehydratases, these two domains reside on separate polypeptide chains, while in type 2 enzymes, they are both found in a single polypeptide. In both the single-chain and two-chain molecules, the catalytic portion is termed the α domain or subunit and the other part the β domain or subunit. In addition, the β domain of *Legionella*

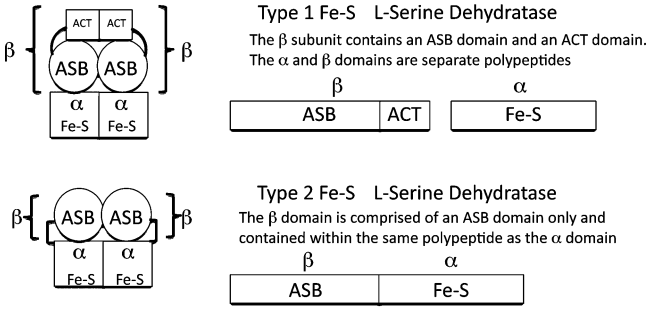

Figure 1. Schematic depiction of type 1 and type 2 L-serine dehydratases. The type 1 enzymes are two chain molecules with the Fe−S center in the α chain and with an ASB and an ACT domain in the β chain. This figure presents the minimal proposed structure. The molecular weight determined for *pa*LSD suggests that two of these units combine to form a hetero-octamer. The type 2 enzymes are single chains that do not contain an ACT domain. The molecular weight of *ec*LSD suggests that it is a dimer as shown. The ASB domain is at the amino termini of both types.

Received: April 23, 2012
Revised: June 4, 2012
Published: June 11, 2012

pneumophila L-serine dehydratase (*lp*LSD), a type 2 enzyme, has recently been shown to possess striking structural homology to the ASB domain of *Mycobacterium tuberculosis* D-3-phosphoglycerate dehydrogenase (*mt*PGDH).[14] ASB stands for "allosteric substrate binding" because it contains a second substrate binding site in *mt*PGDH, where it functions as a codomain, acting in concert with an ACT domain.[15] ACT domains are found in many bacterial proteins and function in the regulation of enzyme activity through interaction with small molecules.[16] In *mt*PGDH, the ASB domain functions as a second site for substrate binding that is necessary for the inhibition of activity resulting from binding of the effector to the ACT domain. The striking structural homology of the β domain of L-serine dehydratases to the ASB regulatory domain in *mt*PGDH suggests that it may also play a regulatory role.

A comparison of the amino acid sequences of representative type 1 and 2 L-serine dehydratases[14] revealed that the type 1 enzymes contain an additional polypeptide segment immediately following the β or ASB domain sequence that displays homology with the ACT domains of phosphoglycerate dehydrogenases.[14] Interestingly, these segments occur in type 1 L-serine dehydratases in the same sequential arrangement that is seen for the tandem ASB and ACT domains in *mt*PGDH, perhaps suggesting a similar regulatory relationship.

The literature regarding the bacterial L-serine dehydratases is not extensive. The most studied are type 2 enzymes from *E. coli*[7,17−20] and type 1 enzymes from *Peptostreptococcus asaccharolyticus*[4−6] and *Clostridium* species.[21,22] Interestingly, the type 1 enzyme from *P. asaccharolyticus* (*pa*LSD) was reported to be a hetero-octamer,[4] while the type 2 enzymes from *E. coli* (*ec*LSD) appear to be homodimers.[7] Therefore, *pa*LSD would presumably have an $\alpha_4\beta_4$ configuration and be twice as large as *ec*LSD with an $(\alpha\beta)_2$ configuration. Because the ACT domains in other proteins are loci for intersubunit association, it is interesting to speculate about whether the putative ACT domains found only in the type 1 enzymes may be responsible for an increased level of subunit association.

Initial studies of *lp*LSD revealed that pyruvate could act as an activator of the enzyme and that it displays competitive kinetics with the substrate, L-serine.[14] This investigation extends these studies with *lp*LSD and contrasts its characteristics with those of the type 1 enzyme from *Bacillus subtilis* (*bs*LSD). The results show that these type 1 and 2 L-serine dehydratases differ significantly in their kinetic characteristics and their sensitivities to oxygen and are sensitive to their ionic environments in remarkably different ways.

EXPERIMENTAL PROCEDURES

The *lp*LSD, with a six-His affinity tag at the amino terminus, was expressed and purified as previously described,[14] except that cobalt-based Talon (Clontech) immobilized metal affinity columns (IMAC) were used instead of nickel-based columns. *bs*LSD was expressed in a pDUET plasmid with the α and β subunits under control of separate promoters. Each subunit was constructed with a six-His affinity tag, with the tag on the amino terminus for the α subunit and on the carboxy terminus for the β subunit. *bs*LSD was also isolated on Talon affinity columns in the same manner as *lp*LSD.

The enzymes were purified and stored under anaerobic conditions using a Coy Laboratories type B anaerobic chamber as previously described.[14] All solutions were sparged with nitrogen, transferred to the anaerobic chamber, and equilibrated with stirring for 24 h before being used. Enzyme samples were removed from the chamber in sealed vials, and aliquots were removed just prior to analysis.

The enzyme activity was determined by following the production of pyruvate at 250 or 360 nm using an extinction coefficient of 93.3 or 6.42 M^{-1} cm^{-1}, respectively. The absorbance at 360 nm in a 0.1 cm cuvette was used for high initial levels of pyruvate. Assays containing sodium iodide were monitored at 280 nm because of the absorbance of sodium iodide at 250 nm. The activity was expressed as the change in absorbance per minute unless otherwise indicated. The concentration of the active enzyme was determined from the absorbance of the iron−sulfur center at 400 nm using an extinction coefficient of 13750 M^{-1} cm^{-1}.[16] Assays were performed in 50 mM NaMOPS buffer (pH 7.0) unless otherwise specified.

The pH versus activity profile was generated using a series of buffers that overlapped at least one pH point with the next to ensure uniformity. Potassium acetate buffer (pH 4.5−5.5), potassium phosphate buffer (pH 5.5−8.0), Tris-HCl buffer (pH 8.0−9.0), and carbonate−bicarbonate buffer (pH 9.0−10.5) were used. The data points were connected with straight lines.

Plots of activity as a function of ion or product concentration were made at low and high L-serine concentrations. For *lp*LSD, the serine concentrations were 2 and 100 mM, and for *bs*LSD, they were 10 and 500 mM. The data were not fit to an equation but simply connected with lines.

Plots of activity versus serine concentration were fit to a form of the Michaelis−Menten equation that incorporates a term for cooperativity

$$v = (V_m[S]^n)/{K_m}^n + [S]^n \quad (1)$$

Nonlinear Lineweaver−Burk plots were fit with a reciprocal form of the equation

$$1/v = (K_m/V_m)(1/[S]^n) + 1/V_m \quad (2)$$

When Lineweaver−Burk plots indicated hyperbolic mixed-type activation, the data were fit to the following equation for that mechanism

$$v = \{V_m([S]/K_m) + \beta V_m[([S][A])/(\alpha K_m K_a)]\}/[1 + [S]/K_m + [A]/K_a + ([S][A])/(\alpha K_m K_a)] \quad (3)$$

where v is the velocity at a given substrate concentration [S] and a given activator concentration [A], V_m is the maximal velocity, K_m is the half-maximal velocity, K_a is the activation constant, β is a coefficient describing the effect of activation on V_m, and α is a coefficient describing the difference in K_m for binding of a substrate to the E and EA forms of the enzyme.

The oxygen sensitivity was monitored after exposure to air by following the enzyme activity after removal of the purified enzymes from the anaerobic chamber. Equal enzyme concentrations (8 μM active site) of *lp*LSD and *bs*LSD were prepared anaerobically and exposed to ambient air by opening the vial to the atmosphere. Monitoring the loss of *bs*LSD activity was completed in 1 day because of the relatively rapid decrease in activity. Monitoring the loss of *lp*LSD activity took place over several days, but assays were not performed during the overnight hours. Plots measuring activity as a function of exposure to air were fit with an equation for a single-exponential process

$$Y = Ae^{(-kt)} + C \quad (4)$$

dx.doi.org/10.1021/bi300523p | *Biochemistry* 2012, 51, 5320−5328

where Y is the relative activity at time t, A is the amplitude, k is the observed rate constant, and C is an offset value. All plots, except where noted, were fit with regression analysis using Kaleidograph version 4.0 from Synergy Software.

RESULTS

Enzyme Expression and Purification. The gene for the type 2 enzyme, *lp*LSD, contains a single reading frame, and the protein is expressed as a single polypeptide containing both the α and β domains. The gene for the type 1 enzyme, *bs*LSD, contains a stop codon between the β and α domains, with the β domain being 5′ to the α domain. Expressing *bs*LSD with a six-His region at the N-terminus of the β subunit results in good isolation of the β subunit but low levels (substoichiometric) of the α subunit. Expressing the β subunit alone does not produce soluble protein, indicating that coexpression of the α subunit is necessary for the folding of the β subunit. On the other hand, the α subunit (containing the [4Fe-S] catalytic center) can be expressed alone and isolated in good yield. However, it does not display any catalytic activity and has an altered spectrum in the 300−450 nm region where the Fe−S center absorbs (Figure S1 of the Supporting Information). Addition of an isolate with stoichiometric excess of β subunits does not restore activity. This may suggest that the presence of the β subunit during expression is necessary for folding or proper formation of the Fe−S center.

Removal of the stop codon between α and β subunits results in no production of soluble enzyme, even when linkers with as many as 10−20 amino acids are added between the two subunit sequences. This most likely indicates that the C-terminus of the β subunit is not in the proximity of the N-terminus of the α subunit in the final oligomer. However, enzyme with high activity is produced by tandem expression of both subunits, each with a six-His extension, in a pDuet vector.

Initially, it was observed that the specific activity of the enzymes was quite variable when isolated with nickel-based affinity columns and that the columns themselves had to be frequently regenerated with nickel. Switching to cobalt-based columns resulted in more reproducible enzyme preparations, and the columns themselves perform well for longer periods of time and do not need regeneration. This is most likely due to the decreased level of leakage of metal from the cobalt Talon columns compared to the nickel columns. The variability in specific activity from batch to batch with nickel columns may be due to partial replacement of iron at the active site with nickel. It was subsequently determined that while both nickel and cobalt inhibit the activity of the L-serine dehydratases, the *lp*LSD enzyme is more sensitive to nickel than to cobalt (Figure S2 of the Supporting Information). Thus, using cobalt-based affinity columns greatly improved the reproducibility of the purification, probably because of a combination of a decreased level of metal leakage and a lower sensitivity to cobalt. Figure 2 shows an SDS gel of *lp*LSD and *bs*LSD isolated with cobalt-based metal affinity columns.

Both enzymes have a relatively broad pH profile (Figure S3 of the Supporting Information), with *lp*LSD being optimally active between pH 5 and 10 and *bs*LSD between pH 6 and 10.

Oxygen Sensitivity. The sensitivity of enzyme activity to oxygen was tested by exposing approximately equimolar enzyme solutions to air and following their decrease in activity with time. *bs*LSD, a type 1 enzyme, was found to be much more sensitive to oxygen than *lp*LSD, a type 2 enzyme (Figure 3). The difference in the rate of activity loss was approximately 30-fold, with *bs*LSD activity being reduced to approximately 15% in 5 h while the *lp*LSD activity took approximately 95 h to reach the same level. No activity could be detected for *bs*LSD after 15 h, while *lp*LSD retained 90% of its activity. The decrease in the activity of *bs*LSD was not affected by the presence of potassium ion (see below).

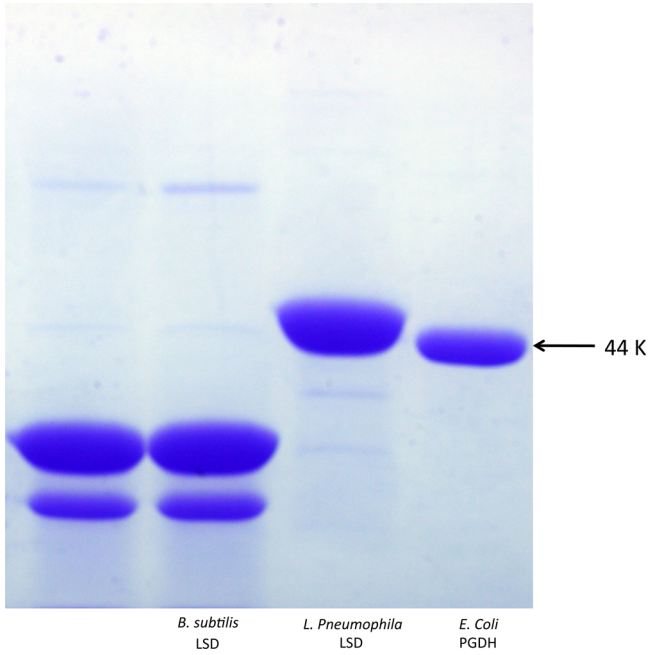

Figure 2. SDS gel of *bs*LSD, *lp*LSD, and *Ec*PGDH. The PGDH is included as a molecular weight marker of 44K.

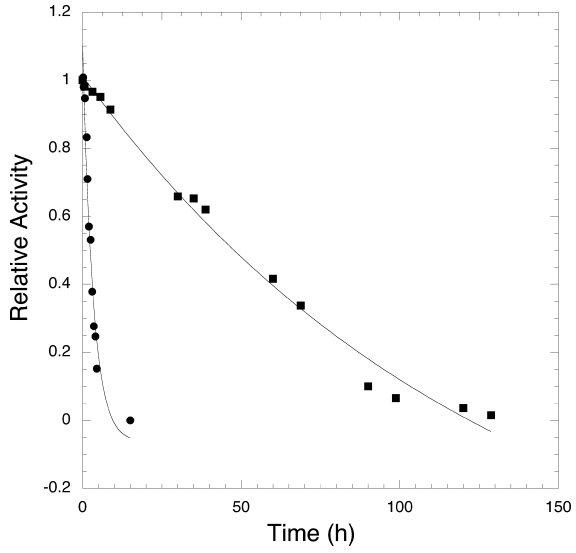

Figure 3. Oxygen sensitivity of *lp*LSD and *bs*LSD. The activity of equimolar amounts of each enzyme was measured as a function of time after passive exposure to air. The data points for *lp*LSD (■) and *bs*LSD (●) are fit to the equation for a single-exponential process (eq 4).

Ion Sensitivity. During the isolation of the type 1 *bs*LSD, it was observed that it possesses very little activity in the absence of potassium ion. In fact, its k_{cat} was approximately 20-fold lower than that observed for *lp*LSD in the same buffer (Table 1). This observation prompted a more comprehensive investigation into the effects of monovalent ions on LSD

dx.doi.org/10.1021/bi300523p | *Biochemistry* 2012, 51, 5320−5328

Table 1. Comparison of Kinetic Parameters of *lp*LSD and *bs*LSD in MOPS Buffer[a]

	K_m (mM)	k_{cat} (s^{-1})	k_{cat}/K_m (M^{-1} s^{-1})	n_H
*lp*LSD	5.1 ± 0.1	286	5.7×10^4	1.41 ± 0.04
*bs*LSD	10.6 ± 3.4	12	0.1×10^4	1.2 ± 0.4
*bs*LSD with 100 mM KCl	13.6 ± 1.1	184	1.4×10^4	1.1 ± 0.1
*bs*LSD with 300 mM KCl	25.5 ± 1.4	465	1.8×10^4	1.1 ± 0.1
*bs*LSD with 500 mM KCl	29.2 ± 2.0	585	2.0×10^4	1.2 ± 0.1

[a]Consisting of 50 mM NaMOPS (pH 7.0).

activity (Figure 4). Both type 1 and type 2 enzymes show the same trend in the effect of monovalent cations. Lithium, in the form of LiCl, has little effect on the activity of *lp*LSD. The same is probably true for *bs*LSD because the enhancement seen for LiCl with this enzyme is probably due to the presence of chloride ion. Sodium has an effect that is intermediate between those of lithium and potassium. The overall effect is larger for *bs*LSD (approximately 20-fold) than for *lp*LSD (approximately 1.2-fold). For both enzymes, the strongest activation is seen with potassium and again much stronger for *bs*LSD. At 100 mM potassium ion, for example, the activity of the type 1 *bs*LSD is enhanced approximately 15-fold compared to only approximately 1.5-fold for *lp*LSD. Furthermore, while the enhancement in activity levels out at this concentration for *lp*LSD, the activity for *bs*LSD continues to increase to approximately 120-fold at 2.75 M potassium chloride. Table 1 shows that the K_m and k_{cat} for *bs*LSD both increase with an increasing potassium concentration. k_{cat}/K_m increases >10-fold in the presence of potassium but then increases only gradually with an increasing potassium concentration, indicating that near-optimal "enzyme efficiency" is achieved at lower potassium ion concentrations. Potassium appears to act as a nonessential activator with both enzymes displaying hyperbolic mixed-type Lineweaver–Burk plots (Figure 5). Fitting of the data to eq 3 for mixed-type hyperbolic activation yields a value for β of 1.57 ± 0.02. This compares very well to the activity enhancement with potassium ion of approximately 1.54 seen in Figure 4 for *lp*LSD.

A differential effect on the two enzymes is also observed with monovalent anions (Figure 4). While chloride ion has little

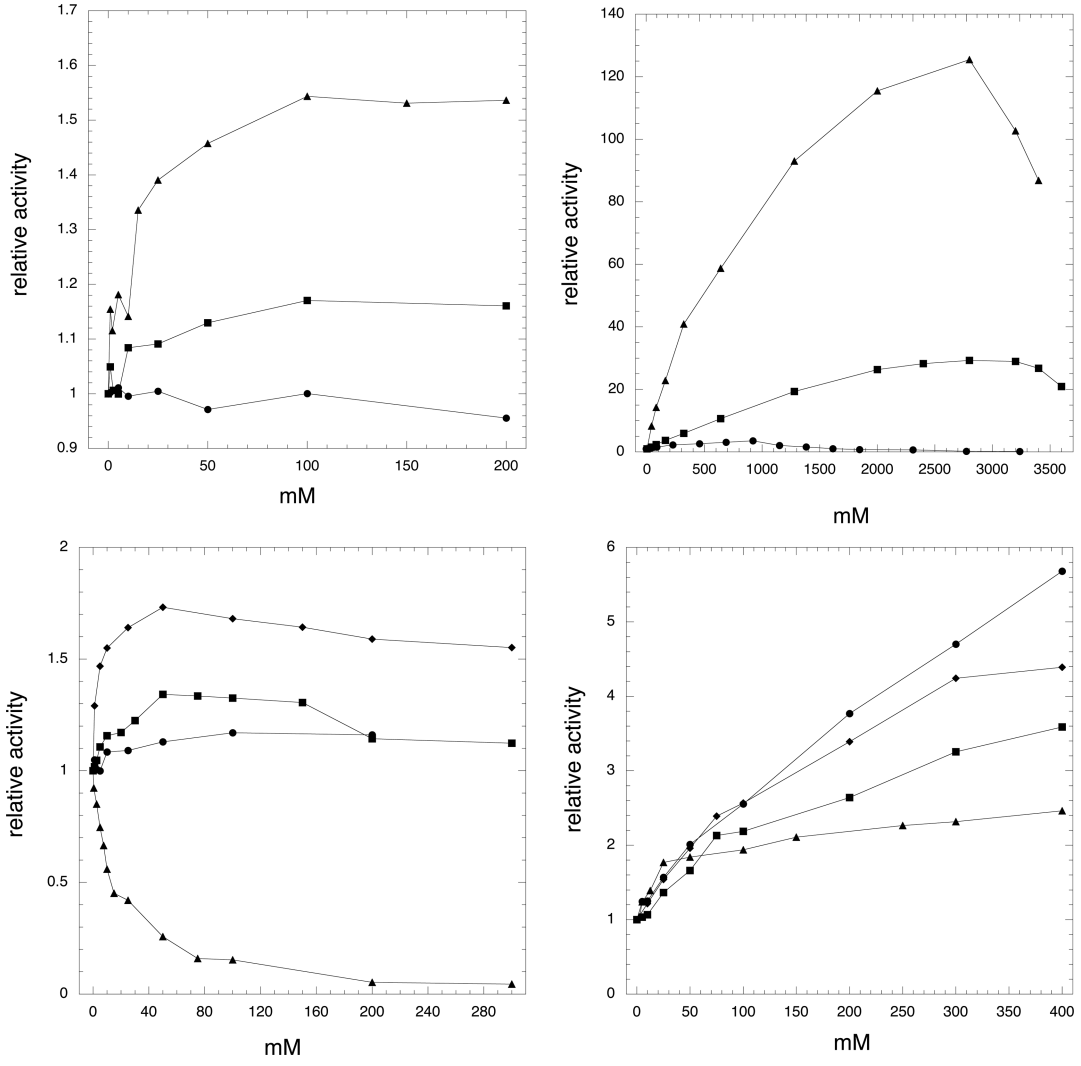

Figure 4. Ion sensitivity of *lp*LSD and *bs*LSD. Data for *lp*LSD are shown in the left panels and those for *bs*LSD in the right panels. Assays were performed in 50 mM NaMOPS (pH 7.0). Bottom panels: NaF (▲), NaCl (●), NaBr (■), and NaI (◆). Top panels: LiCl (●), NaCl (■), and KCl (▲).

dx.doi.org/10.1021/bi300523p | *Biochemistry* 2012, 51, 5320–5328

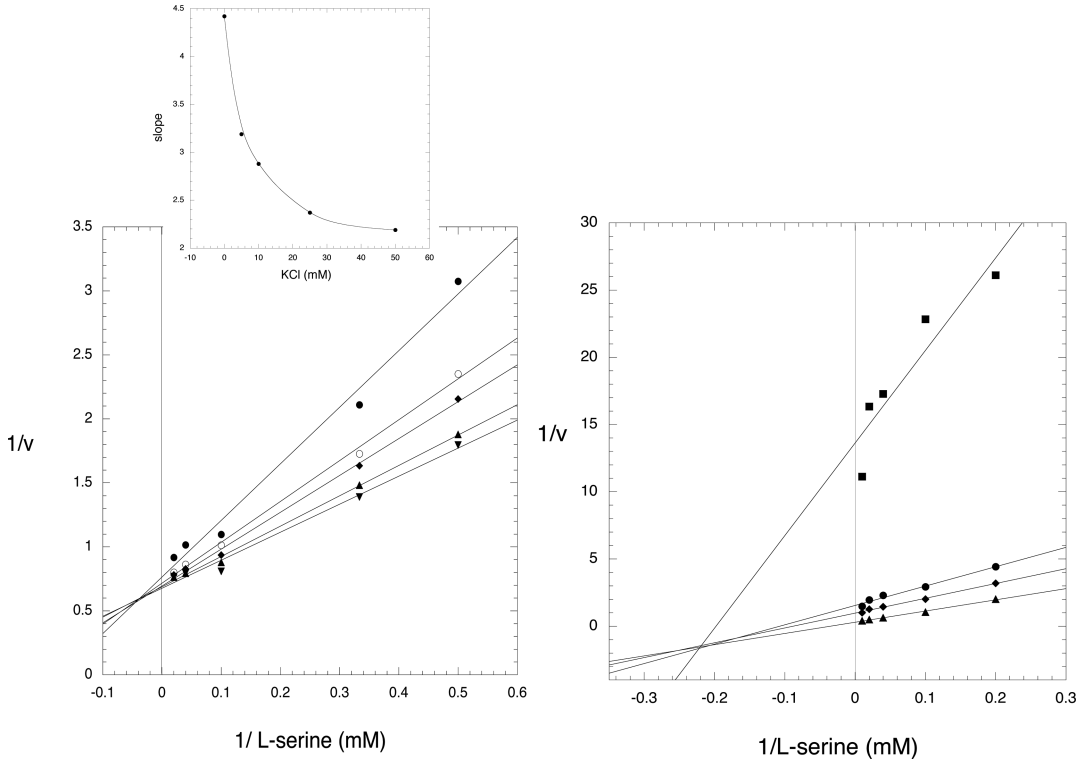

Figure 5. Double-reciprocal plots of the kinetics of KCl. Left: *lp*LSD at 0 (●), 5 (○), 10 (◆), 25 (▲), and 50 mM KCl (▼). The inset shows a plot of the slopes vs KCl concentration. Right: *bs*LSD at 0 (■), 50 (●), 100 (◆), and 500 mM KCl (▲).

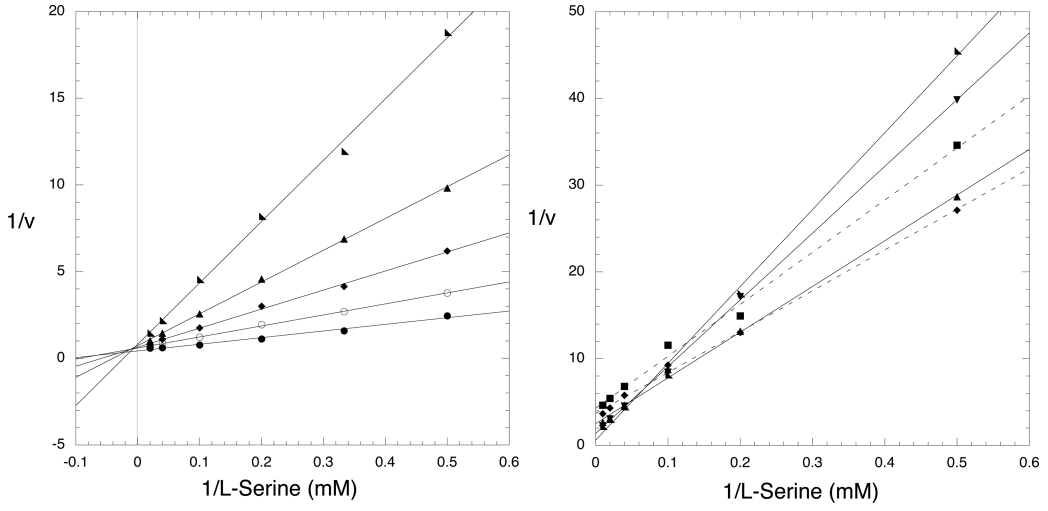

Figure 6. Double-reciprocal plots of the kinetics of NaF. Left: *lp*LSD at 0 (●), 10 (○), 25 (◆), 50 (▲), and 100 mM NaF (right triangles). Right: *bs*LSD at 0 (■), 25 (◆), 100 (▲), 200 (▼), and 250 mM NaF (right triangles). For *bs*LSD in the right panel, the dotted lines show the initial activation followed by the solid lines showing the subsequent inhibition.

effect on *lp*LSD (see LiCl), it is the most effective at stimulating *bs*LSD activity at high concentrations, although the effect at low concentrations is similar to that of fluoride, bromide, and iodide. Fluoride is an effective inhibitor of *lp*LSD. Kinetic analysis (Figure 6) of the effect of NaF on *lp*LSD shows that it is competitive with the substrate, L-serine, with a K_i of approximately 10 mM. On the other hand, low concentrations of flouride ion activate *bs*LSD with apparent competitive kinetics (Figure 6, dashed lines). However, at higher fluoride concentrations, it is an inhibitor at low L-serine concentrations but an activator at high L-serine concentrations. The latter is apparent from the observation that the linear fit of the data intersects to the right of the *y*-axis (Figure 6, solid lines).

Product Activation. It was previously reported that sodium pyruvate activated *lp*LSD at high concentrations in phosphate buffer. In MOPS buffer, the effect is even more pronounced with as much as a 4-fold activation at 200 mM pyruvate (Figure 7). This level of activation cannot be ascribed to the level of sodium present. Furthermore, it is competitive with the substrate L-serine. At 100 mM L-serine, the activation effect is essentially gone and the Lineweaver–Burk plots intersect at the *y* axis. The effect of ammonium chloride on *lp*LSD appears to be somewhat more complex (Figure 8). At low serine

dx.doi.org/10.1021/bi300523p | *Biochemistry* 2012, 51, 5320−5328

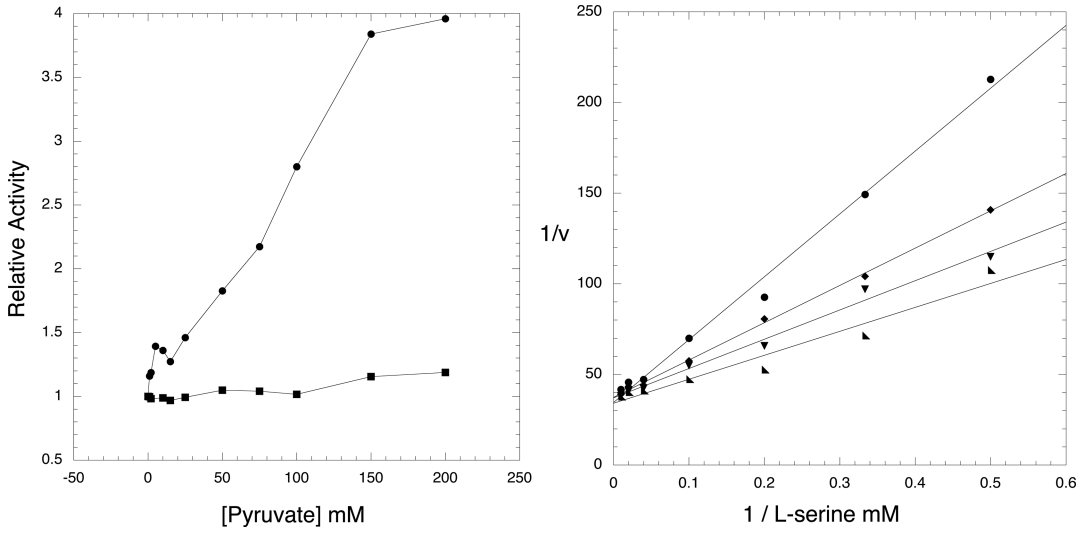

Figure 7. Kinetics of pyruvate activation of *lp*LSD. The left panel shows the relative activity using L-serine concentrations of 2 (●) and 100 mM (■). The right panel is a Lineweaver–Burk plot at varying concentrations of L-serine and various fixed concentrations of pyruvate: 0 (●), 25 (◆), 100 (▼), and 200 mM (right triangles).

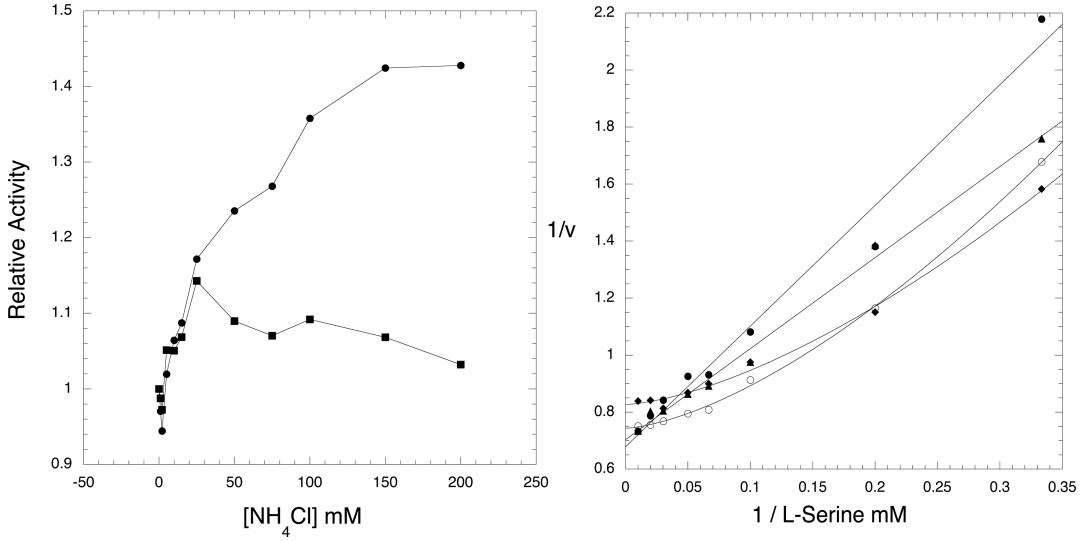

Figure 8. Kinetics of the effect of NH_4Cl on *lp*LSD. The left panel shows the relative activity using L-serine concentrations of 2 (●) and 100 mM (■). The right panel is a Lineweaver–Burk plot at varying concentrations of L-serine and various fixed concentrations of NH_4Cl: 5 (●), 25 (▲), 80 (○), and 200 mM (◆).

concentrations, there is a slight enhancement in activity. At high serine concentrations, there is an initial enhancement of activity followed by inhibition above approximately 25 mM ammonium chloride. Because chloride appears to have no effect on *lp*LSD, this is probably due to the ammonium ion, although the magnitude is relatively low. The Lineweaver–Burk plot reflects these observations. At low ammonia concentrations, the data are best fit to a straight line, while at higher concentrations, the fit becomes distinctly nonlinear. At all concentrations of ammonia though, the activation changes to inhibition at high serine concentrations.

The effect of ammonium ion on *bs*LSD is significantly different (Figure 9). While it is also slightly activating, it is not particularly sensitive to serine concentration, although there is a small difference between low and high serine levels up to ~200 mM ammonium chloride. The activation appears to be essentially noncompetitive, particularly at higher concentrations.

For *bs*LSD, pyruvate is initially an inhibitor at low concentrations but then produces an apparent small activation at higher pyruvate concentrations. As is the case for *lp*LSD, the action of pyruvate is competitive with L-serine for *bs*LSD, as well. However, the subsequent pyruvate activation of *bs*LSD restores activity only to the level found in the absence of pyruvate.

■ DISCUSSION

The bacterial L-serine dehydratases are only the second type of enzyme shown to possess a unique structural motif, termed the ASB domain. This domain bears its name because it acts as an allosteric substrate binding site in the only other protein in which it has been found, *M. tuberculosis* D-3-phosphoglycerate dehydrogenase. As part of an effort to determine if the ASB domain serves the same function or a similar function in L-serine dehydratases, this investigation comprises a detailed look at the catalytic and kinetic characteristics of two L-serine

dx.doi.org/10.1021/bi300523p | *Biochemistry* 2012, 51, 5320–5328

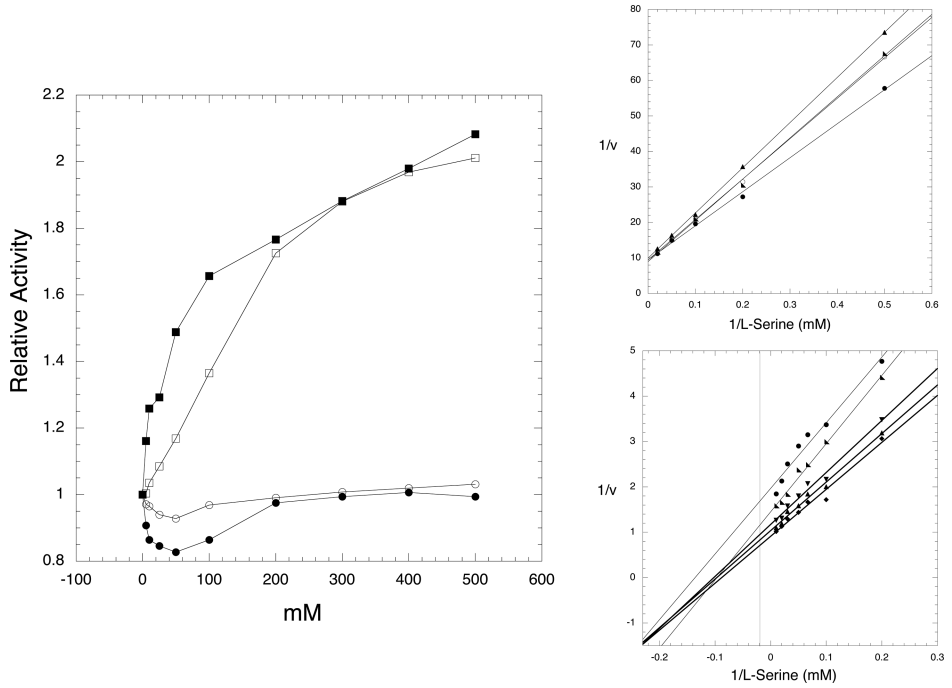

Figure 9. Kinetics of the effect of pyruvate and NH_4Cl on *bs*LSD. The left panel shows the relative activity for NH_4Cl with L-serine concentrations of 10 (■) and 500 mM (□) and for pyruvate with L-serine concentrations of 10 (●) and 500 mM (○). The top right panel shows the Lineweaver–Burk plot for varying L-serine concentrations at various fixed concentrations of pyruvate: 0 (●), 10 (○), 50 (▲), and 200 mM (right triangles). The bottom right panel shows the Lineweaver–Burk plot for varying L-serine concentrations at various fixed concentrations of NH_4Cl: 0 (●), 25 (right triangles), 100 (▼), 150 (▲), and 200 mM (◆).

dehydratases that represent each of the two structurally distinct types and reveals that they also display distinctly contrasting properties.

The expression of *lp*LSD and *bs*LSD with six-His tags and the isolation on cobalt-based metal affinity columns produce a highly pure enzyme with consistent levels of specific activity. Although it is difficult to compare the specific activities between these enzymes because of the differential effects on the activity of monovalent ions and products, it is clear that both are highly active enzymes with k_{cat} values exceeding 200 s^{-1}.

It is equally clear that they are distinctly different enzymes. This is seen first in the differences in their subunit conformation.[4,7] The type 2 enzymes are expressed as single chains, while the type 1 enzymes are expressed as two separate chains. In the type 1 enzymes, the subunit containing the ASB domain also contains an ACT domain in the same tandem orientation as seen in *mt*PGDH. Given that ACT domains tend to form homodimers in most known structures,[16] these domains may be responsible for higher-order association like that reported for *pa*LSD.[4] The presence of the ACT domain may also be why the type 1 enzymes evolved to be expressed as two separate polypeptides. That is, the position of the ACT domain in the gene sequence may not be compatible with its protein surface being properly positioned to form a dimer interface if it connects directly to the α subunit. This notion is consistent with the observation that no protein product can be detected when the stop codon between the two subunits is removed so that a single chain would be expressed. This conformational concept is represented schematically in Figure 1, where the ASB domain–α subunit contacts are conserved and the ACT domain is positioned on the opposite side of the ASB domain from the α subunit. Confirmation of this hypothesis will require that their respective structures be determined and their association states determined by size exclusion chromatography or analytical ultracentrifugation.

A distinct difference is also seen in their sensitivity to oxygen. The sensitivity of iron–sulfur centers to oxygen has been described well,[1,2] with aconitase being the prototypical [4Fe-4S] enzyme. The remarkable difference in the rate of decay of activity upon exposure to oxygen between the two enzyme types suggests a significant difference in the structure around the iron–sulfur center that affects the accessibility of the center to oxygen.

Both enzymes are activated by cations, with the larger ones being more effective. Lithium appears to give no significant activation. Potassium activates both enzymes at relatively low concentrations, and the magnitude of the activation can be very large for the type 1 *bs*LSD. The inhibition observed at higher concentrations may be due to the anion. Thus, it is possible that the cation produces more activation than the anion produces inhibition, and the inhibition is not observed until the activation process is saturated. Anions appear to inhibit, with the smaller being more effective. Overall inhibition is not observed except in the case of fluoride for *lp*LSD, but the effect for the other anions could be masked by opposite activation by cations. Fluoride inhibition of *lp*LSD is strictly competitive with L-serine but complex and mixed for *bs*LSD, again suggesting different mechanisms.

Pyruvate appears to be a product inhibitor for *lp*LSD because it is competitive with L-serine. However, it produces activation of the enzyme that is not compatible with it simply competing for binding at the active site. Furthermore, the level of activation appears to be greater than what would be expected from the sodium counterion alone. This observation suggests the presence of a second site for pyruvate where it exerts an allosteric effect on activity. Because the activation can be

dx.doi.org/10.1021/bi300523p | *Biochemistry* 2012, 51, 5320–5328

eliminated by higher levels of L-serine, it may be that this second site is actually a second serine binding site. This idea is consistent with the ASB domain containing a substrate binding site that participates in allosteric control similar to that seen for the ASB domain in *tb*PGDH.

Activation of *lp*LSD with ammonia is likely due to a cation effect, but inhibition is observed at higher L-serine concentrations. The Lineweaver–Burk plots suggest a complex pattern and probably reflect the fact that ammonia is both a cation activator and a product or dead-end inhibitor where the inhibition reflects the binding of ammonia to an enzyme form present at saturating L-serine concentrations.

The product interaction patterns for *bs*LSD are again quite different. Pyruvate is not a potent activator but does show characteristics of being competitive with L-serine and binding to a second site at high concentrations. Ammonia activation is not competitive with L-serine and appears to be mainly noncompetitive as the ammonia concentration increases. These observations are also consistent with ammonia interacting with different forms of the enzyme, possibly at two different sites.

While the opposing sensitivities to cations and anions tend to complicate the kinetic interpretations, the data indicate the presence of a second site for pyruvate binding that may, in fact, be weakly interacting with what is actually a second serine binding site. This idea is consistent with the presence of an ASB domain acting in a manner similar to that in *tb*PGDH. Also very interesting are the requirement of *bs*LSD for potassium ion and its activation over a very wide range of concentrations. This may reflect a very high K_d for potassium ion and may somehow be linked with bacterial cellular potassium levels. It is clear that potassium has a very profound effect on enzyme activity. Even with a high K_d, the enzyme could have a significant occupancy of potassium at lower millimolar concentrations of ion if the initial binding is followed by a conformational transition to a tight binding form where the forward rate of the transformation is significantly greater than the reverse rate.

The bacterial L-serine dehydratases seem to occupy a unique biological niche based on their contrasting mechanism compared to mammalian serine dehydratases and bacterial D-serine dehydratases. While the substrates and products are the same, mammalian L- and D-serine dehydratases, as well as bacterial D-serine dehydratases, employ a pyridoxyl phosphate prosthetic group, while the bacterial L-serine dehydratases utilize an iron–sulfur center.

The characteristics of these enzymes bring up several obvious questions. One question is why the K_m values for L-serine are so high. In light of the recent evidence that these enzymes function in controlling or preventing high L-serine levels in the context of cell wall synthesis, the relatively high K_m values are not unreasonable. The enzymes would display relatively low activity at low serine concentrations so that the serine pool would not be completely depleted but would experience increases in activity as serine concentrations increased. The intracellular serine concentration would not necessarily have to reach the K_m or beyond for them to be effective in controlling the cellular flux of serine.

Another question concerns the biological reason for the utilization of an Fe–S center rather than pyridoxyl phosphate. Embedded in that question is yet another layer of complexity. Why are there two different types of Fe–S-based L-serine dehydratases that display remarkable differences in structure and catalytic characteristics? The answer to this last question may be associated with the observation that the two types show significant phylogenetic segregation. Although a rigorous informatic study has not yet been conducted, it has been noted[14] that the type 1 enzymes predominate in Firmicutes species that are generally Gram-positive while the type 2 enzymes predominate in Proteobacteria that are generally Gram-negative. The different characteristics could be linked to differences in the cellular environment or a requirement for different levels of control of L-serine in relation to cell wall synthesis. In any case, this investigation provides the first detailed description of the catalytic characteristics of bacterial L-serine dehydratases and provides a basis for further investigation into their actual physiological role in bacterial metabolism.

■ ASSOCIATED CONTENT

Supporting Information

pH dependence, inhibition by cobalt and nickel, and UV spectra of active and inactive α subunits. This material is available free of charge via the Internet at http://pubs.acs.org.

■ AUTHOR INFORMATION

Corresponding Author

*Department of Developmental Biology, Box 8103, Washington University School of Medicine, St. Louis, MO 63110. Phone: (314) 362-3367. Fax: (314) 362-4698. E-mail: ggrant@wustl.edu.

Notes

The authors declare no competing financial interest.

■ ACKNOWLEDGMENTS

We thank Dr. Paul F. Cook for many helpful discussions and for providing insight into the kinetics. We thank Dr. Petra A. Levin for the wild-type *B. subtilis* DNA.

■ ABBREVIATIONS

PGDH, phosphoglycerate dehydrogenase; LSD, L-serine dehydratase; ASB, allosteric substrate binding; ACT, Asp kinase, chorismate mutase, TyrA.

■ REFERENCES

(1) Beinert, H., Kennedy, M. C., and Stout, C. D. (1996) Aconitase as iron-sulfur protein, enzyme, and iron-regulatory protein. *Chem. Rev. 96*, 2335–2373.

(2) Flint, D. H., and Allen, R. M. (1996) Iron-Sulfur Proteins with Nonredox Functions. *Chem. Rev. 96*, 2315–2334.

(3) Grabowski, R., Hoffmeister, A. E. M., and Buckel, W. (1993) Bacterial L-serine dehydratases: A new family of enzymes containing iron-sulfur clusters. *Trends Biochem. Sci. 18*, 297–300.

(4) Grabowski, R., and Buckel, W. (1991) Purification and Properties of an Iron-Sulfur Containing and Pyridoxyl Phosphate-Independent L-Serine Dehydratase from *Peptostreptococcus asaccharolyticus*. *Eur. J. Biochem. 199*, 89–94.

(5) Hoffmeister, A. E. M., Albracht, S. P. J., and Buckel, W. (1994) Iron-Sulfur Cluster Containing L-Serine Dehydratase from *Peptostreptococcus asaccharolyticus*: Correlation of the Cluster Type with Enzymatic Activity. *FEBS Lett. 351*, 416–418.

(6) Hoffmeister, A. E. M., Textor, S., and Buckel, W. (1997) Cloning and Expression of Two Genes Coding for L-Serine Dehydratase from *Peptostreptococcus asaccharolyticus:* Relationship of the Iron-Sulfur Protein to Both L-Serine Dehydratases from *Escherichia coli*. *J. Bacteriol. 179*, 4937–4941.

(7) Cicchillo, R. M., Baker, M. A., Schnitzer, E. J., Newman, E. B., Krebs, C., and Booker, S. J. (2004) *Escherichia coli* L-Serine

Dehydratase Requires a [4Fe-4S] Cluster in Catalysis. *J. Biol. Chem. 279*, 32418−32425.
(8) Purich, D. L., and Allison, R. D. (2002) *The Enzyme Reference: A comprehensive guide to enzyme nomenclature, reactions, and methods*, Academic Press-Elsevier Science, New York.
(9) Voet, D., and Voet, J. G. (2011) *Biochemistry*, 4th ed., John Wiley and Sons, New York.
(10) Frederiuk, C. S., Bayer, R., and Shafer, J. A. (1983) Characterization of the Catalytic Pathway for D-Serine Dehydratase. *J. Biol. Chem. 258*, 5379−5385.
(11) Cheung, Y.-F., and Walsh, C. (1976) Sterospecific Synthesis of Isotopically Labeled Serine at Carbon 3 and Stereochemical Analysis of D-Serine Dehydratase Reaction. *J. Am. Chem. Soc. 98*, 3397−3398.
(12) Zhang, X., and Newman, E. (2008) Deficiency in L-serine deaminase results in abnormal growth and cell division of *Escherichia coli* K-12. *Mol. Microbiol. 69*, 870−881.
(13) Zhang, X., El-Hajj, Z. W., and Newman, E. (2010) Deficiency of L-serine deaminase interferes with one-carbon metabolism and cell wall synthesis in *Escherichia coli* K-12. *J. Bacteriol. 192*, 5515−5525.
(14) Xu, X. L., Chen, S., and Grant, G. A. (2011) Kinetic, Mutagenic, and Structural Homology Analysis of L-Serine Dehydratase from *Legionella pneumophila*. *Arch. Biochem. Biophys. 515* (1−2), 28−36.
(15) Burton, R. L., Chen, S., Xu, X. L., and Grant, G. A. (2009) Role of the anion-binding site in catalysis and regulation of *Mycobacterium tuberculosis* D-3-phosphoglycerate dehydrogenase. *Biochemistry 48*, 4808−4815.
(16) Grant, G. A. (2006) The ACT domain: A small molecule binding domain and its role as a common regulatory element. *J. Biol. Chem. 281*, 33825−33829.
(17) Su, H., Lang, B. F., and Newman, E. B. (1989) L-Serine Degradation in *Escherichia coli* K-12: Cloning and Sequencing of the *sdaA* Gene. *J. Bacteriol. 171*, 5095−5102.
(18) Shao, Z., and Newman, E. B. (1993) Sequencing and Characterization of the *sdaB* Gene from *Escherichia coli* K-12. *Eur. J. Biochem. 212*, 777−784.
(19) Burman, J. D., Harris, R. L., Hauton, K. A., Lawson, D. M., and Sawers, R. G. (2004) The iron-sulfur cluster in the L-serine dehydratse TdcG from *Escherichia coli* is required for enzyme activity. *FEBS Lett. 576*, 442−444.
(20) Su, H., and Newman, E. B. (1991) A novel L-serine deaminase activity in *Escherichia coli* K-12. *J. Bacteriol. 173*, 2473−2480.
(21) Carter, J. E., and Sagers, R. D. (1972) Ferrous Ion-Dependent L-Serine Dehydratase from *Clostridium acidiurci*. *J. Bacteriol. 109*, 757−763.
(22) Hofmeister, A. E. M., Grabowski, R., Linder, D., and Buckel, W. (1993) L-Serine and L-threonine dehydratse from *Clostridium propionicum*: Two enzymes with different prosthetic groups. *Eur. J. Biochem. 215*, 341−349.